

# Analysis of the space-time microstructure of cosmic ray air showers using the HADES RPC TOF wall

---

**Daniel Belver<sup>a,1</sup>, Alberto Blanco<sup>b</sup>, Pablo Cabanelas<sup>a,2</sup>, José Díaz<sup>c</sup>, Paulo Fonte<sup>b,d</sup>, Juan A. Garzón<sup>a</sup>, Alejandro Gil<sup>c,3</sup>, Diego González-Díaz<sup>e,4</sup>, Wolfgang Koenig<sup>e</sup>, Burkhard Kolb<sup>e</sup>, Georgy Kornakov<sup>a,b,\*</sup>, Luís Lopes<sup>b</sup>, Marek Palka<sup>f</sup>, Americo Pereira<sup>b</sup>, Michael Traxler<sup>e</sup>, Peter Zumbruch<sup>e</sup>**

<sup>a</sup>*LabCAF, Universidade de Santiago de Compostela, USC, Santiago de Compostela, Spain*

<sup>b</sup>*Laboratorio de Instrumentação e Física Experimental de Partículas, LIP, Coimbra, Portugal*

<sup>c</sup>*Instituto de Física Corpuscular, IFIC, Valencia, Spain*

<sup>d</sup>*ISEC-Instituto Superior de Engenharia de Coimbra, Coimbra, Portugal*

<sup>e</sup>*GSI Helmholtzzentrum für Schwerionenforschung GmbH, Darmstadt, Germany*

<sup>f</sup>*Smoluchowski Institute of Physics, Jagiellonian University of Cracow, Poland*

<sup>1</sup> *Presently at ESS-Bilbao, Zamudio, Spain*

<sup>2</sup> *Presently at GENP, Universidade de Santiago de Compostela, Santiago de Compostela, Spain*

<sup>3</sup> *Presently at Kirchhoff-Institute for Physics, Heidelberg, Germany*

<sup>4</sup> *Presently at Laboratorio de Física Nuclear y Altas Energías, Universidad de Zaragoza, Zaragoza, Spain*

*E-mail: georgui.kornakov@usc.es*

**ABSTRACT:** Cosmic rays have been studied, since they were discovered one century ago, with a very broad spectrum of detectors and techniques. However, never the properties of the extended air showers (EAS) induced by high energy primary cosmic rays had been analysed at the Earth surface with a high granularity detector and a time resolution at the 0.1 ns scale. The commissioning of the timing RPC (Resistive Plate Chambers) time of flight wall of the HADES spectrometer with cosmic rays, at the GSI (Darmstadt, Germany), opened up that opportunity. During the last months of 2009, more than 500 millions of cosmic ray events were recorded by a stack of two RPC modules, of about 1.25 m<sup>2</sup> each, able to measure swarms of up to  $\sim 100$  particles with a time resolution better than 100 ps. In this document it is demonstrated how such a relative small two-plane, high-granularity timing RPC setup may provide significant information about the properties of the shower and hence about the primary cosmic ray properties.

**KEYWORDS:** Resistive-plate chambers; Timing detectors; cosmic ray showers; Linsley scheme.

---

\*Corresponding author.

---

## Contents

1. Introduction	1
2. Setup description, calibration and synchronisation	1
3. Results	3
4. Summary and discussion	6

---

## 1. Introduction

The HADES (High-Acceptance DiElectron Spectrometer) spectrometer at GSI-SIS [1] was upgraded in 2009[2] in order to allow exploration of the dielectron production channel in heavy nuclei collisions. For such a purpose, an inner TOF wall based on shielded timing RPCs [3] was designed[4], built and finally commissioned in a cosmic ray test [5].

Recent studies propose to use RPC-based detectors as tracking and timing devices in order to measure cosmic ray showers [6][7]. In this paper the performance of the HADES RPCs as a detector with capability to analyse both time and position microstructure of cosmic ray showers has been assessed. Among  $\sim 600$  Mevent recorded, a selection of  $\sim 40$  Mevent, corresponding to a five days continuous run under stable conditions, has been chosen for analysis. The mean trigger rate was around  $100 \text{ Hz/m}^2$ . A description of all the calibration and synchronization procedures, track candidate finder and some analysis results are presented.

## 2. Setup description, calibration and synchronisation

The HADES RPC wall was designed to optimize the performance of the spectrometer in high multiplicity environments. A total area of  $7.5 \text{ m}^2$ , covering the six sectors ( $1.25 \text{ m}^2$  each) of the spectrometer, comprises 1116 individually shielded cells of 4-gap timing RPCs. Each sector is distributed in two layers with three columns and 31 cells (rows) within each column [2] as it is shown in Fig.1(a). Both layers are overlapped in a 40% of their surface. Each cell has two readout channels, left and right, which provide both time and charge information through a charge to width (Q2W) method. The time and x-position observables are obtained as:

$$t_{rpc} = \frac{1}{2}(t_{left} + t_{right}), \quad (2.1)$$

$$x_{rpc} = \frac{1}{2}(t_{left} - t_{right})v_{prop}, \quad (2.2)$$

where  $t_{left/right}$  is the time measured by the left or right channel respectively and  $v_{prop}$  is the signal propagation velocity in the cell. The  $y_{rpc}$  is given by the y-coordinate in the center of each cell.

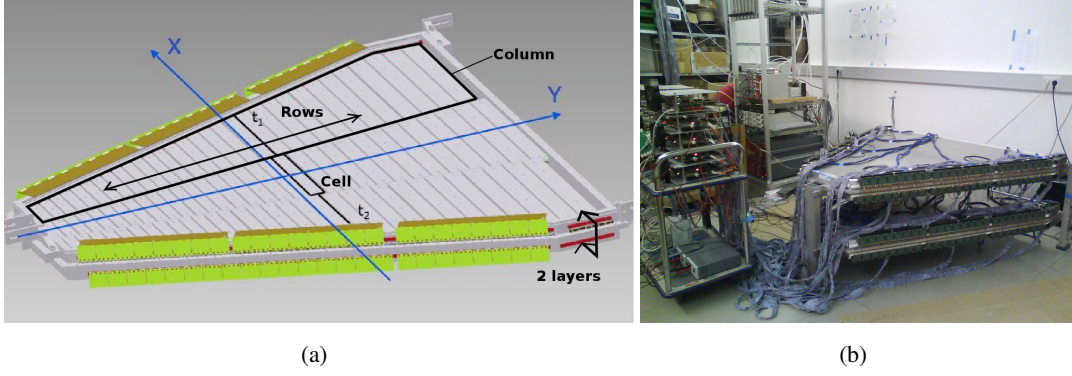


**Figure 1.** a) Schematic layout of the detector. RPC shielded cells distribution in rows, columns, layers and reference coordinates are shown. b) Two HADES RPC sectors taking cosmic ray data during the commissioning of the detectors.

During the cosmic test, pairs of two sectors were stacked horizontally at a distance of 350 mm as it is shown in Fig.1(b). Detectors were operated indoors under a couple of light roofs offering less than one radiation length width to the incoming showers. The reported average time resolution for individual cells was 77 ps rms width and the x-axis reconstructed position resolution was below 12 mm rms width over all cells [5]. The resolution in  $y_{rpc}$  is given by geometry, ranging from  $22/\sqrt{12}$  mm rms width to  $50/\sqrt{12}$  mm rms width. In the case that two hits, belonging to overlapped columns, have compatible time and position (both within  $3\sigma$ ) they are clustered in one hit with the consequent resolution improvement.

Charge and position calibration tasks were carried out using events with less than four fired cells in each sector in order to avoid contamination by multiple hits. Position and charge observables were calibrated by setting constant offsets in the measured values.

Events with one traceable particle crossing both sectors of the stack were required for synchronisation purposes. To enhance the probability of choosing a good particle candidate, the position difference between both hits belonging to overlapped layers was required to remain within  $3\sigma$ .

The trigger was defined by the coincidence of the upper and the lower sectors. Each recorded event has its own time reference and only relative times between hits are available. Therefore, the full detector synchronisation was achieved using a recursive algorithm that minimises the time differences between the two sectors. Under the hypothesis that all particles travel at the speed of light,  $c$ , time difference between hits should fulfil:

$$\Delta T = (t_{rpc-i} - \tau_i)|_{down} - (t_{rpc-j} - \tau_j)|_{up} - d_{ij}/c = 0, \quad (2.3)$$

where  $d_{ij}$  is the distance between hits of cell  $i$  and  $j$  and  $\tau_{i,j}$  is the time offset of the respective cell.  $\Delta T$  has been minimised iteratively and convergence was reached after 5 iterations over all cells. By characterising the  $\Delta T$  distribution a criteria for selecting track candidates can be derived. The standard deviation ( $\sigma_T$ ) was found to be  $\sim 176$  ps rms width. The distribution and the fit are shown in Fig.2. In the shower front analysis,  $\Delta T$  between hits was required to be always within  $3\sigma$  to define a track candidate. Each track is characterised by the arrival time,  $t_{rpc}$  and  $(x_{rpc}, y_{rpc})$  coordinates in the upper plane and an unit vector  $\mathbf{n}_i = (\alpha_i, \beta_i, \gamma_i)$  in the propagation direction.

Fig.3 shows an example of a reconstructed high multiplicity event where the reconstructed track candidates are represented by arrows.

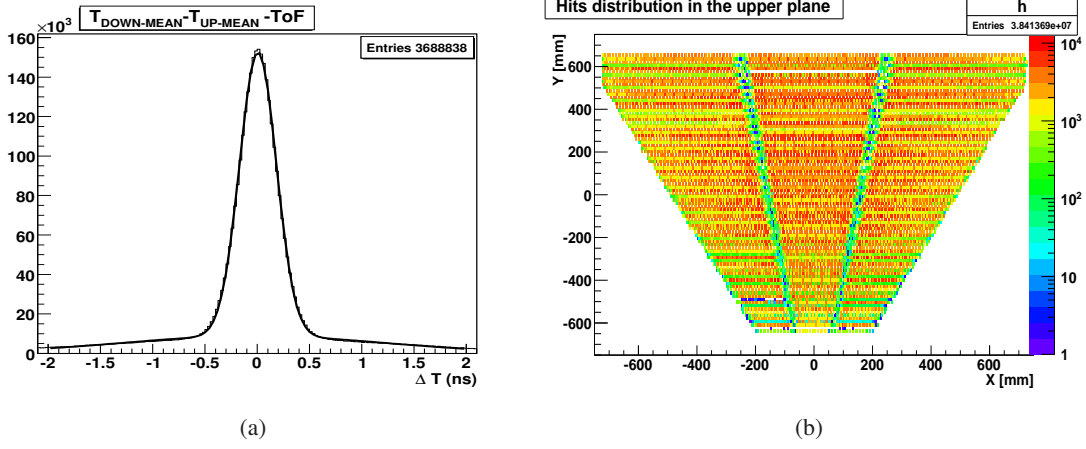


**Figure 2.** a)  $\Delta T$  distribution between the upper and the lower sectors. Two gaussians have been fitted to interpret both signal and background. The rms of the signal is 176.45 ps. b) Hit distribution at the upper sector after the position calibration. The three-column structure of the detector and the different cells sizes are apparent.

After reconstructing tracks, we define the shower's incidence angle  $\mathbf{n}_s = (\alpha_s, \beta_s, \gamma_s)$  as:

$$\mathbf{n}_s = \frac{\sum_{i=1}^{N_{tracks}} \mathbf{n}_i \cdot w_i}{\left| \sum_{i=1}^{N_{tracks}} \mathbf{n}_i \cdot w_i \right|}, \quad (2.4)$$

where  $N_{tracks}$  is the number of track candidates and  $w_i = \sigma_T / (\sigma_T + \Delta T_i)$  is a weight factor, being  $\Delta T$  defined in the equation 2.3. The introduction of a weight factor is mandatory because, in high multiplicity events, the asymmetric acceptance of the detector may introduce systematic deviations in the incidence angle reconstruction. Once an estimate of the arrival direction of the shower has been calculated, the corrected arrival time is defined as:

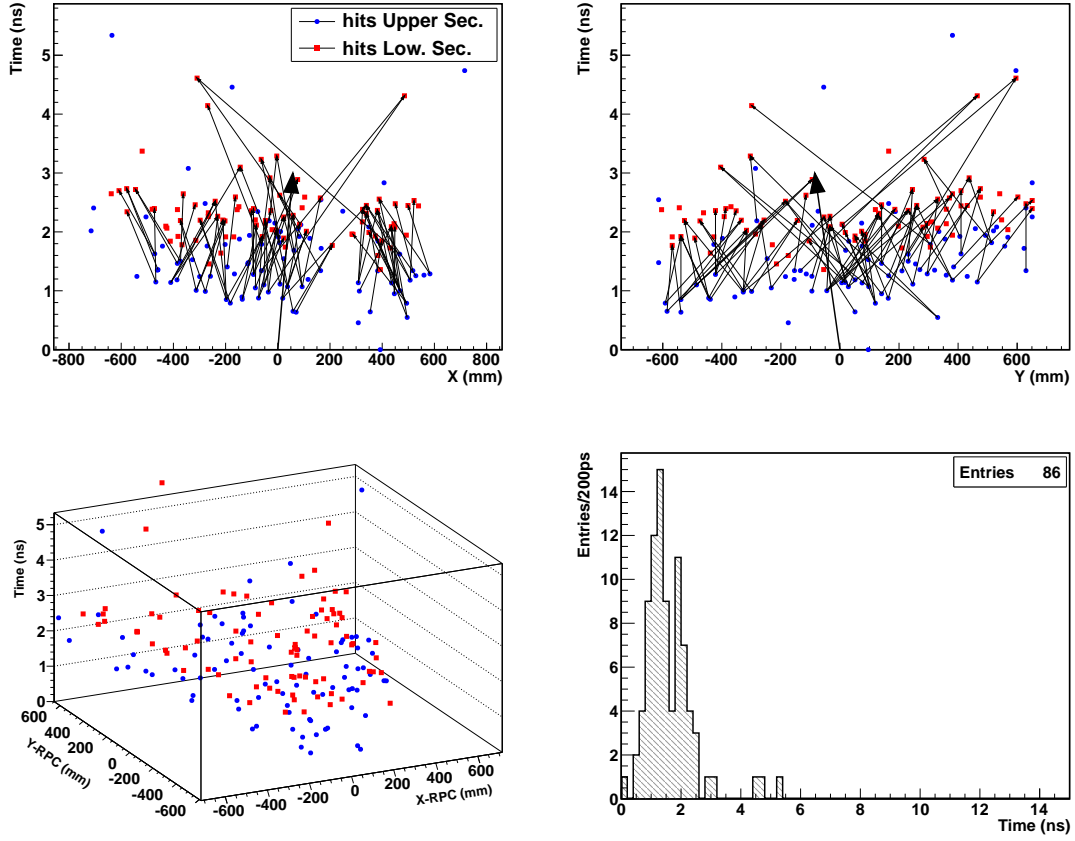
$$t_{corr} = t_{rpc} - (\alpha_s \cdot x_{rpc} + \beta_s \cdot y_{rpc}) \cdot c^{-1}. \quad (2.5)$$

Fig. 3 shows an example of the reconstructed incidence direction and time profile after the aforementioned correction.

### 3. Results

In this section results informing about the low scale structure of showers measured are presented. No correction related to geometry, efficiency, dead time, occupancy or acceptance has been performed, although any of these factors could affect significantly our qualitative results.

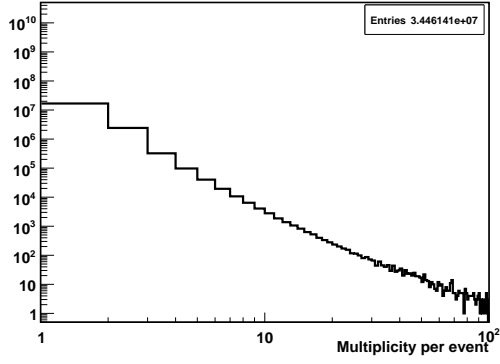
The hit multiplicity of the events in the sample is shown in Fig.4(a). Fig.4(b) shows the mean charge of the hits in the upper sector as a function of the multiplicity of the showers. The



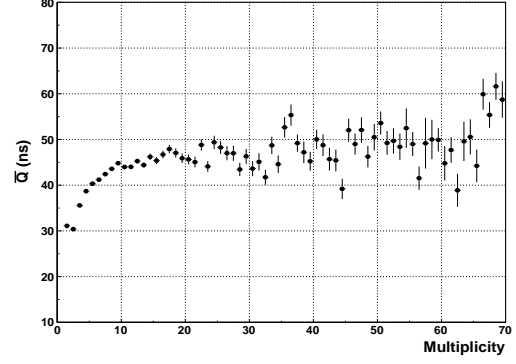
**Figure 3.** Example of the arrival profile of a high multiplicity shower after calibration and synchronisation. Blue and red markers refer to the top and bottom sectors respectively. A delay of around  $\sim 1$  ns due to 350 mm separation between them is observable. Arrows represent the track and shower directions. Top left:  $t_{rpc}$  vs  $x_{rpc}$ -coordinate. Top right:  $t_{rpc}$  vs  $y_{rpc}$ -coordinate. Bottom left: 3D view of the measured particles. Bottom right: Profile of arrival time after performing the incidence angle correction.

observed increase of the mean charge with the multiplicity may be explained as a consequence of the detected particle type, since in general cosmic electrons are more ionizing particles than cosmic muons. Therefore, it shows how low multiplicity events are mainly dominated by muons whereas the electron content increases together with the multiplicity.

Fig.5(a) shows the number of events as a function of both the hit multiplicity and the time width of the front, defined as the standard deviation of corrected arrival times of particles in the shower. Roughly, higher multiplicities correspond to higher energy primaries and larger time widths correspond to higher distances between the detector and the core of the shower [8]. Then, low energy showers tend to occupy the bottom-left corner of the figure whereas very much less frequent high energy shower tend to occupy the upper-right corner. Fig.5(b) shows in the z-axis the mean charge per event. Here the well known effect that for high multiplicity/energy showers, the electromagnetic component dominates near the core (bottom-right side), whereas the muonic component dominates far away from the core (upper-left side), can be seen. Also, low energy showers are mainly populated by muons.

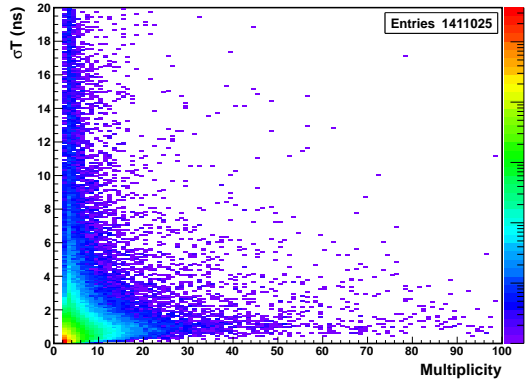


(a)

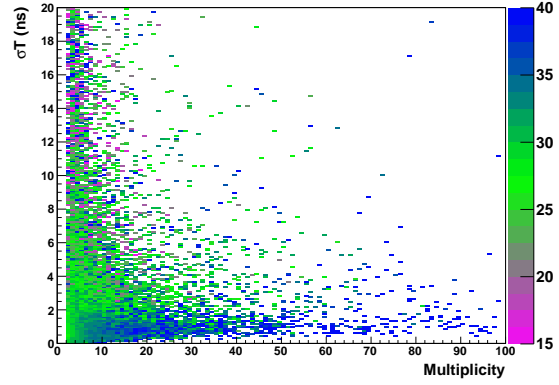


(b)

**Figure 4.** a) Measured multiplicity in the upper sector of all the triggered events over a continuous five day period. b) Mean measured charge as a function of multiplicity for all the events with at least one track candidate.



(a)



(b)

**Figure 5.** a) Scatter plot of multiplicity vs the standard deviation of arrival times within a shower. b) Same plot representing in the z-axis the mean measured charge.

Fig.6 shows the corrected time delay of the hits in the upper sector respect to the first arriving particle for several multiplicity selections. Lower multiplicity distributions show several changes of slopes that would need further analysis. However, a few general conclusions can be extracted. Low multiplicity distributions are mainly dominated by low-energy showers, having particles arriving with very short time differences of 1-2 ns. As the multiplicity increases the slope of the distributions decrease, showing the effect that high multiplicity events are increasingly dominated by showers of higher energies arriving far away from the detector. Large time differences correspond to particles of high energy showers having arrived very far away from the detector. The high multiplicity subsample shows the gamma-like distribution already observed in high energy showers [9].

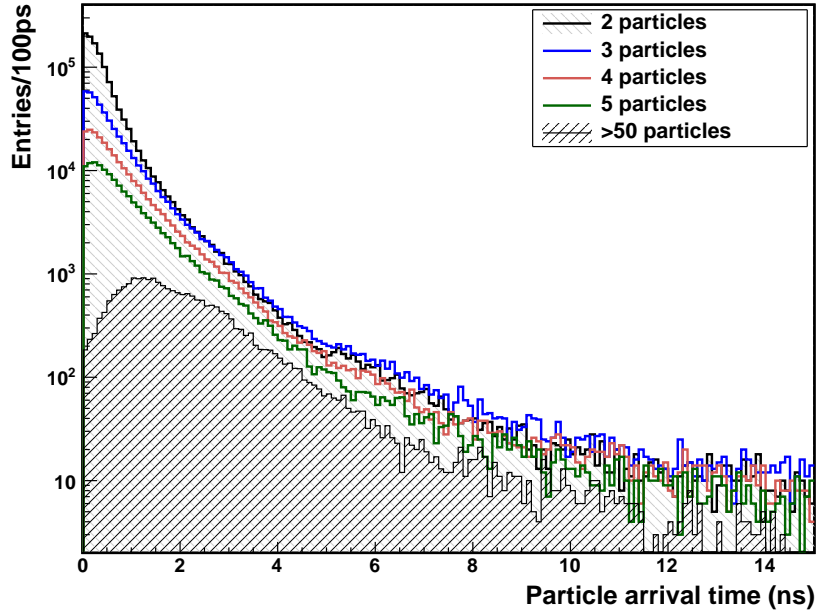


**Figure 6.** Arrival time of all the hits within a shower referred to the first measured time for several multiplicity selections. Neither geometry, efficiency, dead time nor acceptance corrections have been included.

#### 4. Summary and discussion

The previous results show that a detector composed by several planes of high granularity timing RPCs may provide access, at the same time, to a wide range of cosmic rays observables at an affordable price: particle density, arrival time distribution, electron/muon ratio or local arrival direction. All this variables may give faithful information about the properties of the parent primary cosmic ray.

Primary cosmic rays above an energy of about  $E \sim 10^{15}$  eV are so scarce that their main properties (mass, energy and arrival direction) have to be estimated indirectly measuring a small sample of the billions of secondary particles produced when they interact with the atoms of the atmosphere. For this purpose secondaries are gathered using big arrays of detectors placed at the Earth surface, big enough to cover the whole swarm of particles. However, other alternatives have been proposed.

J.Linsley suggested in the eighties [10] to use the empirical relationships observed in the showers relating the time width with the distance to the core and the particle density at this distance with both the size of the shower and the energy. Using this features, a mini array of detectors able to measure the density and the arrival time distribution of particles could be used to measure the rarest and more energetic cosmic rays. A network of such small arrays, working independently of each other, could be an alternative to the big arrays of detectors at a less cost per unit area.

The Linsley's approach has been used by different experiments as Akeno [16] [15], the GU mini-array [11] [12] and LAAS [13] [17] to analyze cosmic rays. All of them provided results that



are in agreement with those provided by observatories using traditional techniques. More recent studies [8] show that electrons and muons behave very differently far away from the core, both in their arrival time and in their time distribution. A separate parameterization of these effects should allow to improve substantially the method.

Other initiative, the NEVOD-DECOR complex, has started to study extended air showers using a single big-volume ( $2000 \text{ m}^3$ ) detector based on the measurement of other observables as the local muon density and the energy of the muon bundles. This experiment show how a single experimental setup gives the possibility to study features of the spectrum and the composition of primary cosmic rays and characteristics of hadron interaction in a wide energy range [14].

In this regard, timing RPC-based detectors providing:

- a) a good granularity for the measurement of the particle density
- b) a very good time resolution for the accurate measurement of the time profile and, together with a), providing an estimate of the energy of the shower
- c) the tracking of all the charged particles and an estimate of the local direction of the shower, allowing the time distribution correction,
- d) an estimate of the electron/muon ratio and estimates of their respective arrival time distributions and densities,

together with all the correlations among them, could offer a new way to analyze cosmic ray showers as an alternative to other methods. Such kind of detectors could be also of interest for complementing traditional big-array observatories or big-volume facilities.

Results presented in this article are very encouraging. However more work should be necessary to analyze the possibility of improving the capability of RPCs to separate cosmic electron and muons via either an appropriate tuning of the operational parameters or improving the charge sampling using more layers. Also, more detailed and accurate studies about the relationship between the micro-structure of the front region of a shower and the primary cosmic ray parameters provided by an external big observatory should be performed.

## References

- [1] P. Salabura, et al., *Probing of in-medium hadron structure with HADES*, *Nucl. Phys. A* **749** (2005) 150.
- [2] D. Belver et al., *The HADES RPC inner TOF wall*, *Nucl. Instr. and Meth. A* **602** (2009) 687.
- [3] Ch. Finck, et al., *Results concerning understanding and applications of timing GRPCs*, *Nucl. Instr. and Meth. A* **508** (2003) 63.
- [4] H. Alvarez Pol et al., *A large area timing RPC prototype for ion collisions in the HADES spectrometer*, *Nucl. Instr. and Meth. A* **535** (2004) 277.
- [5] A. Blanco, et al., *RPC HADES-TOF wall cosmic ray test performance*, *Nucl. Instr. and Meth. A* **661** (2012) S114.
- [6] P. Assis, et al., *R&D for an autonomous RPC station*, *32nd. Intern. Cosmic Ray Conf.*, Beijing (2011).
- [7] D. Belver, et al., *TRASGO: A proposal for a timing RPCs based detector for analyzing cosmic ray air showers*, *Nucl. Instr. and Meth. A* **661** (2012) S163.
- [8] W.D. Apel et al. *Time structure of the EAS electron and muon components measured by the KASCADE-Grande experiment*, *Astropart. Phys.* **29** (2008) 317-330.



- [9] G. Agnetta et al., *Time structure of the extensive air shower front*, *Astropart. Phys.* **6** (1997) 301-312.
- [10] J. Linsley, *Mini and super mini arrays for the study of highest energy cosmic rays*, *19th Intern. Cosmic Ray Conf., La Jolla* (1985) 3, 434-437
- [11] T. Bezboruah, K. Boruah, P.K. Boruah, *A non conventional method of UHE cosmic ray detection*, *Astropart. Phys.* **11** (1999) 395-402.
- [12] U.D. Goswami, K. Boruah and P.K. Boruah, *New results from Gauhati University miniarray detector*, *29th. Intern. Cosmic Ray Conf., Pune* (2005) 7, 159-162.
- [13] H. Matsumoto et al., *Simulation studies and implementation of Linsley's EAS time structure method for the primary cosmic ray spectrum*, *Nucl. Instr. and Meth. A* **614** (2010) 475-482
- [14] I.I. Yashin et al., *Investigation of primary cosmic ray spectrum shape by means of EAS muon density technique*, *European Cosmic Ray Symposium, Kosice* (2008).
- [15] W.E. Hazen, H.Y. Dai and E.S. Hazen, *Study of a mini-array for the Linsley effect in cosmic-ray air showers*, *J. Phys. G: Nucl. Part. Phys.* **15** (1989) 113.
- [16] M. Teshima et al., *Properties of  $10^9$ - $10^{10}$  GeV extensive air showers at core distances between 100 and 3000 m*, *J. Phys. G: Nucl. Part. Phys.* **12** (1986) 1097.
- [17] A. Iyono et al., *Linsley's EAS time structure method for the primary cosmic ray spectrum at LAAS*, *Astrophys. Space Sci. Trans.*, **7** (2011) 335